Jurnal Penginderaan Jauh dan Pengolahan Data Citra Digital Vol. 19 No. 1
*ISSN: 1412-8098 (print), 2549-726X (online)*

# Analysis of $SO_2$ Emissions and Thermal Anomalies from the Eruption of Mount Lewotobi Laki-laki in November 2024 Using Google Earth Engine

**Febryanto Pratama [a,*], Lalu Muhamad Jaelani [a]**
[a] Department of Geomatics Engineering, Institut Teknologi Sepuluh Nopember, Surabaya 60111, Indonesia

*Corresponding author: febryantopratama0@gmail.com

**Abstract.** Mount Lewotobi is one of the active volcanoes located in Wulanggitang District, East Flores Regency, East Nusa Tenggara. Mount Lewotobi Laki-Laki in November 2024 has been detected showing significant volcanic activity. This volcanic activity has been detected emitting volcanic gas emissions and significant lava flows that could affect air quality, structures, and the surrounding ecosystem. In this study, we aim to evaluate $SO_2$ emissions from Sentinel-5P Tropospheric Monitoring Instrument (TROPOMI) and hotspot area produced by lava eruption using Sentinel-2 Multispectral Imager (MSI) and Landsat-8 Operational Land Imager (OLI). Data processing was conducted using the Google Earth Engine platform to obtain spatial and temporal analyses of $SO_2$ concentrations in the air and heat sources. The Normalized Hotspot Indices (NHI) method was applied to identify and map hotspots generated by volcanic activity. Through the implementation of a combination computation process that incorporates $SO_2$ measurements alongside the detection of hotspots, this method has demonstrated a high degree of effectiveness in analyzing the effects of eruptions by utilizing remote sensing techniques.The study shows that the highest $SO_2$ levels showed a maximum value of 300.831 µg/m³ and an average of 71.928 µg/m³ occurring on November 9, 2024, which was the highest peak of the eruption. The classification of hotspot distribution indicated a range from high temperature intensity to low temperature intensity. The elevated concentration of $SO_2$ observed in the vicinity of the volcanic eruption can be attributed to the significant saturation of sulfur dioxide present in the atmosphere. The total number of hotspots measured was 51 hot pixels on Landsat-8 and 278 hot pixels on Sentinel-2. The statistical test results for Landsat-8 data showed no significant correlation between $SO_2$ measurements and hotspot measurements, whereas the results for Sentinel-2 showed an inverse correlation. A high number $SO_2$ of and hotspots pose a potential threat not only to vegetation, but also the well-being of the local population.

**Keywords:** Air Quality, Google Earth Engine, Normalized Hotspot Indices (NHI), Remote Sensing, Sulfur Dioxide ($SO_2$), Thermal Areas, Volcanic Emissions,

## I. INTRODUCTION

Indonesia, located along the Pacific Ring of Fire, is one of the most volcanically active regions in the world, with more than 120 active volcanoes [1]. This volcanic activity periodically poses a serious threat to environmental quality, particularly through the emission of harmful gases such as sulfur dioxide ($SO_2$). These gases can reduce air quality, endanger human health, and disrupt the balance of ecosystems. One recent event of concern was the eruption of Mount Lewotobi Laki-Laki in East Nusa Tenggara in November 2024, which produced large amounts of $SO_2$ emissions accompanied by intense thermal anomalies. This event underscores the need for spatial and temporal monitoring of the environmental impacts of volcanic activityThe introduction should provide a comprehensive background of the problem under investigation, including relevant issues and a review of prior research conducted by other investigators. This section should also highlight the distinctions, advantages, and objectives of the present study.

Previous studies have demonstrated the usefulness of satellite remote sensing in monitoring volcanic $SO_2$ emissions and thermal anomalies. For example, [2] used Sentinel-5P Tropospheric Monitoring Instrument (TROPOMI) data to assess $SO_2$ emissions from the Hunga Tonga eruption, which showed a significant increase in $SO_2$ concentrations during the event. Similarly [3] developed Normalized Hotspot Indices (NHI) algorithms using Sentinel-2 and Landsat-8 data to detect volcanic thermal anomalies with promising accuracy at various volcanoes around the world. Meanwhile, [4] introduced a machine learning technique for $SO_2$ plume classification using TROPOMI data, improving the accuracy and efficiency of volcanic emission monitoring. However, few studies have combined both approaches simultaneously for a specific eruption event. Additionally, validation methods using external sources such as Middle InfraRed Observation of Volcanic Activity (MIROVA) or $SO_2$ measurement data from NASA have not been widely implemented, particularly for eruptions in Indonesia. This opens up opportunities for further exploration.

Despite advances in satellite-based observation technology, the main challenge that remains is the lack of integration between volcanic gas monitoring and thermal anomalies within a single comprehensive framework. Most studies still focus on only one aspect, without examining the relationship or correlation between the two. Additionally, the operational use of cloud computing platforms such as Google Earth Engine (GEE) in the context of Indonesia for volcanic disaster monitoring remains limited. Most studies only focus on gas emissions or thermal anomalies separately, with limited efforts to explore their correlation or validate combined analyses using field data. The utilization of platforms such as GEE for operational monitoring and validation is still underutilized in the Indonesian regional context.

This study proposes an integrated approach by combining satellites data such as Sentinel-5P Tropospheric Monitoring Instrument (TROPOMI), Sentinel-2 Multispectral Imager (MSI), and Landsat-8 Operational Land Imager (OLI) data on the Google Earth Engine platform to assess the spatial and temporal distribution of $SO_2$ and thermal anomalies caused by the eruption of Mount Lewotobi Laki-Laki in November 2024. The Normalized Hotspot Indices (NHI) method is utilized for the detection of thermal anomalies caused by lava eruptions. The implementation of this method relies on the utilization of multispectral imager and operational land imager data. Additionally, the analysis results will be validated using external data such as Middle InfraRed Observation of Volcanic Activity (MIROVA) and NASA's $SO_2$ data to enhance the accuracy and reliability of the research findings.

This study uses a cloud computing approach with the Google Earth Engine platform to integrate data from Sentinel-5P, Sentinel-2, and Landsat-8. Google Earth Engine facilitates expeditious, scalable spatial analysis by providing cloud-based access to large geospatial datasets and sophisticated built-in tools, thereby eliminating the necessity for local storage and computing resources. The platform facilitates collaboration, reproducibility, and advanced analytics, including machine learning, thereby enhancing the efficiency and accessibility of complex analyses across extensive regions. $SO_2$ detection is performed from the TROPOMI (Tropospheric Monitoring Instrument) ultraviolet channel [5] while thermal anomalies are calculated using the NHI index based on infrared data from MSI and OLI. Spatial-temporal correlation analysis was conducted to evaluate the relationship between gas emission intensity and thermal activity. This approach is expected to provide a more comprehensive understanding of the environmental impact of volcanic activity and support the development of a more responsive and data-driven volcanic disaster monitoring system. This research offers a new approach that combines gas emission monitoring and thermal activity in a single integrated system, which has not been widely applied in the Indonesian context. This integration not only enhances the effectiveness of volcanic disaster monitoring but can also be applied in near real-time and on a large scale through Google Earth Engine. The contributions of this research are expected to strengthen early warning systems and data-driven decision-making for mitigating the impacts of volcanic eruptions, as well as serve as a reference for similar studies in other disaster-prone regions.

## II. METHODOLOGY

### *2.1 Study Area*

This study focuses on Mount Lewotobi Laki-Laki, located in East Nusa Tenggara Province, Indonesia (approximately at coordinates 8.543° S and 122.777° E), with an estimated elevation of 1,584 meters, including a ±400 meters crater. The region is characterized by a high incidence of explosive eruptions, elevated seismic activity, and the occurrence of pyroclastic flows. These geologic phenomena have a significant impact on the local community, often necessitating evacuation and prolonged displacement of nearby populations. The population within a 7 km radius of the site is approximately 16,000. The eruption occurred in November 2024 and produced large amounts of volcanic gas emissions and thermal energy. Recent eruptions have led to the displacement of thousands of individuals, with a peak displacement of up to 13,000 km at one point. The time period studied in this research covers November 1 to 30, 2024, to capture the pre-eruption, eruption, and post-eruption phases. The location of the study and the scope of the observation area are shown in Figure 1.

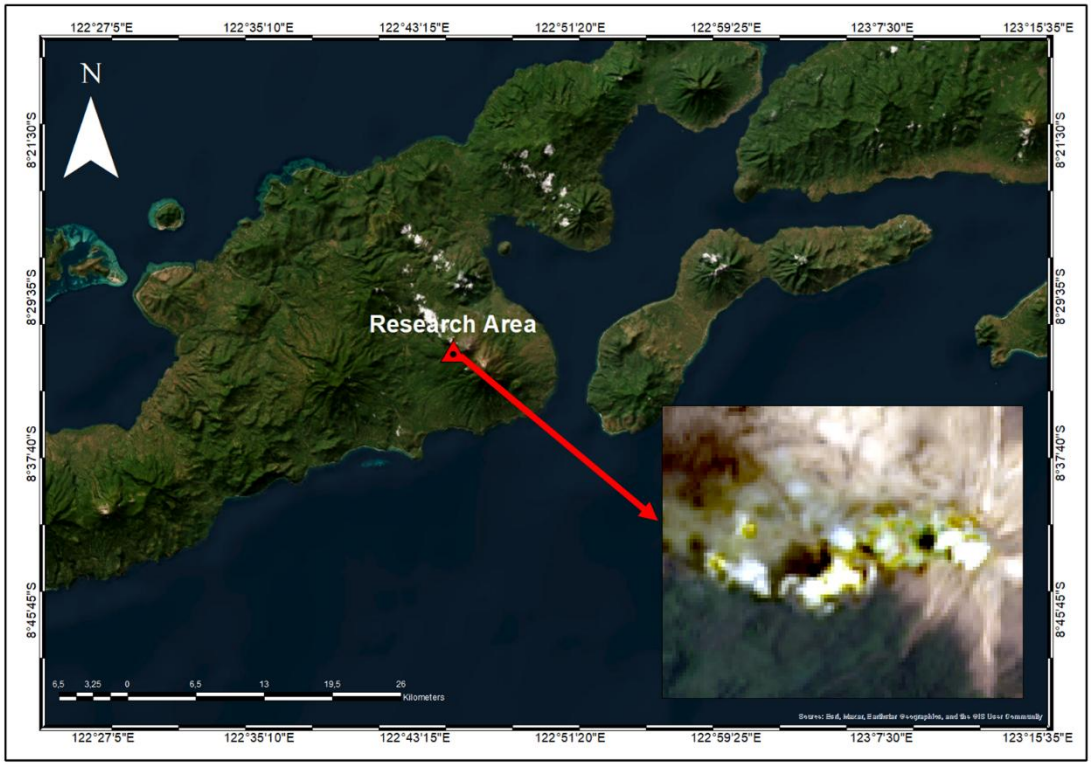


Figure 1. Research Area

## 2.2 *Methods and Data*

This study uses remote sensing data, namely Sentinel-5P, Sentinel-2, and Landsat-8, to detect $SO_2$ in the atmosphere and detect thermal anomalies on the Earth's surface spatially and temporally during the eruption of Mount Lewotobi Laki-Laki in November 2024, all of which were accessed and analyzed using the GEE platform. The application of the Normalized Hotspot Indices (NHI) algorithm requires multispectral data comprising shortwave infrared (SWIR) and near-infrared (NIR) to effectively identify thermal anomalies and active hotspot regions. The Multispectral Instrument (MSI) onboard Sentinel-2 and the Operational Land Imager (OLI) onboard Landsat-8 both provide these spectral bands with adequate spatial resolution (ranging from 10 to 30 meters) and consistent radiometric quality, making them suitable for detailed hotspot analysis. SWIR bands (approximately 1.5–2.5 µm) are particularly valuable for detecting high-temperature features such as active fires, volcanic hotspots, and thermal anomalies. This is due to the fact that hot surfaces emit significant radiation in this range and SWIR reflectance is less affected by atmospheric scattering. Conversely, near-infrared bands (approximately 0.8–1.0 µm) exhibit a high degree of sensitivity to vegetation structure and moisture content, thereby rendering them indispensable for the mapping of vegetation health and the discrimination of land cover types. When combined in indices like the Normalized Hotspot Indices (NHI), the SWIR and NIR bands complement each other by enhancing the detection of thermal anomalies while simultaneously suppressing background noise from vegetation or soil. This improves the reliability of hotspot detection in complex environments.

### *2.2.1 Sentinel-5P (TROPOMI)*

Sentinel-5P data from the TROPOMI sensor was used to detect volcanic gas emissions, particularly $SO_2$, produced during the eruption phase. Sentinel-5P provides daily data with a spatial resolution of approximately 7 × 3.5 km, and the product used in this study was Level-2 offline $SO_2$, which includes the total vertical column of $SO_2$ (unit: mol/m²). To ensure data quality, filtering was performed based on cloud fraction and quality value (qa_value), with only data having a quality value above 0.5 being used in the analysis. Sentinel-5P itself acquires data daily, enabling it to provide high-quality global data [6].

### *2.2.2 Sentinel-2 (MSI)*

Sentinel-2 data, equipped with MSI (Multispectral Instrument) sensors, is used to detect thermal anomalies through NHI calculations to determine hot

spots or areas of the Lewotobi Laki-Laki volcano eruption. This index is calculated using a combination of Band 8 (Near Infrared/NIR) and Band 12 (Shortwave Infrared/SWIR), which have spatial resolutions of 10 and 20 meters, respectively. This approach follows the method developed by [7], which demonstrated the effectiveness of NHI in identifying volcanic thermal anomalies with high accuracy in various volcanic regions around the world. Sentinel-2 was chosen because of its high acquisition frequency, wide spatial coverage, and ability to detect spectral changes in the surface caused by extreme thermal activity in detail [8]. In this study, Sentinel-2 images were selectively taken on days when there were indications of thermal anomalies based on reports from monitoring systems such as MIROVA [9]

*2.2.3 Landsat-8 (OLI)*

Landsat-8 data was used to support the detection of thermal anomalies related to the eruption of Mount Lewotobi Laki-Laki. This satellite has two main instruments, namely the Operational Land Imager (OLI) and Thermal Infrared Sensor (TIRS), which enable the acquisition of high-quality multispectral and thermal data with a 16-day repeat cycle [10], [11]. In this study, data processing was performed using the NIR (Near Infrared) and SWIR (Shortwave Infrared) bands from Landsat-8 imagery, each with a spatial resolution of 30 meters. Both bands were used to calculate the NHI to identify hotspots or areas associated with thermal activity from the eruption of Mount Lewotobi Laki-Laki. The use of this method is in line with recent research by[11], which demonstrates the effectiveness of using Landsat-8 data for monitoring thermal anomalies in active volcanic areas.

*2.3 Data Processing*

The methodology outlined in this study summarizes the main steps in data processing and analysis. The diagram shows the integration of data from Sentinel-5P for monitoring sulfur dioxide ($SO_2$) emissions, as well as Sentinel-2 and Landsat-8 for mapping thermal anomalies. All processing stages were carried out systematically on the GEE platform, which enables efficient and large-scale spatial data processing. The complete flow of the research stages is shown in Figure 2.

These measurements are characterized by their high temporal resolution and global coverage, both of which are indispensable for the effective monitoring of atmospheric trace gases. These measurements, initially reported in mol per square meter ($mol/m^2$), are systematically converted to micrograms per cubic meter ($\mu g/m^3$) to align with standard air quality assessment metrics. Subsequent to this initial step, the system performs a calculation to determine the spatial distribution of $SO_2$ concentrations. Then, classification techniques are applied to distinguish between different concentration levels across the study area. Subsequently, temporal analysis is conducted to capture trends, fluctuations, and potential emission events over time.

Spatial-temporal analysis was conducted to observe the distribution patterns and intensity of gas plumes during the eruption period. Meanwhile, thermal anomaly mapping was performed using the NHI algorithm. This algorithm is a multi-channel method that utilizes shortwave infrared (SWIR) and near-infrared (NIR) channels to identify areas showing significant thermal activity [12]. The outputs are then mapped using geospatial technology and, when feasible, compared to ancillary data or historical records for validation. The utilization of GEE cloud-based computational framework enables the efficient processing of voluminous temporal stacks of imagery, thereby facilitating near-real-time monitoring and comprehensive spatial analysis of thermal anomalies across extensive regions. In its implementation, the NHI algorithm consists of two main equations: NHIswnir and NHIswir, each tailored to the wavelength of the MSI and OLI sensors. Equations (1) and (2) below show how the index is calculated based on Top of Atmosphere Reflectance (TOA) in each channel. These indices leverage the substantial thermal emissivity of active hotspots, where heightened SWIR reflectance signifies elevated surface temperatures. Normalization serves to mitigate the impact of background reflectance variability. Consequently, the NHI algorithm effectively enhances the contrast between hotspot pixels and surrounding areas, thereby supporting accurate and scalable detection of thermal anomalies in applications such as volcanic monitoring.

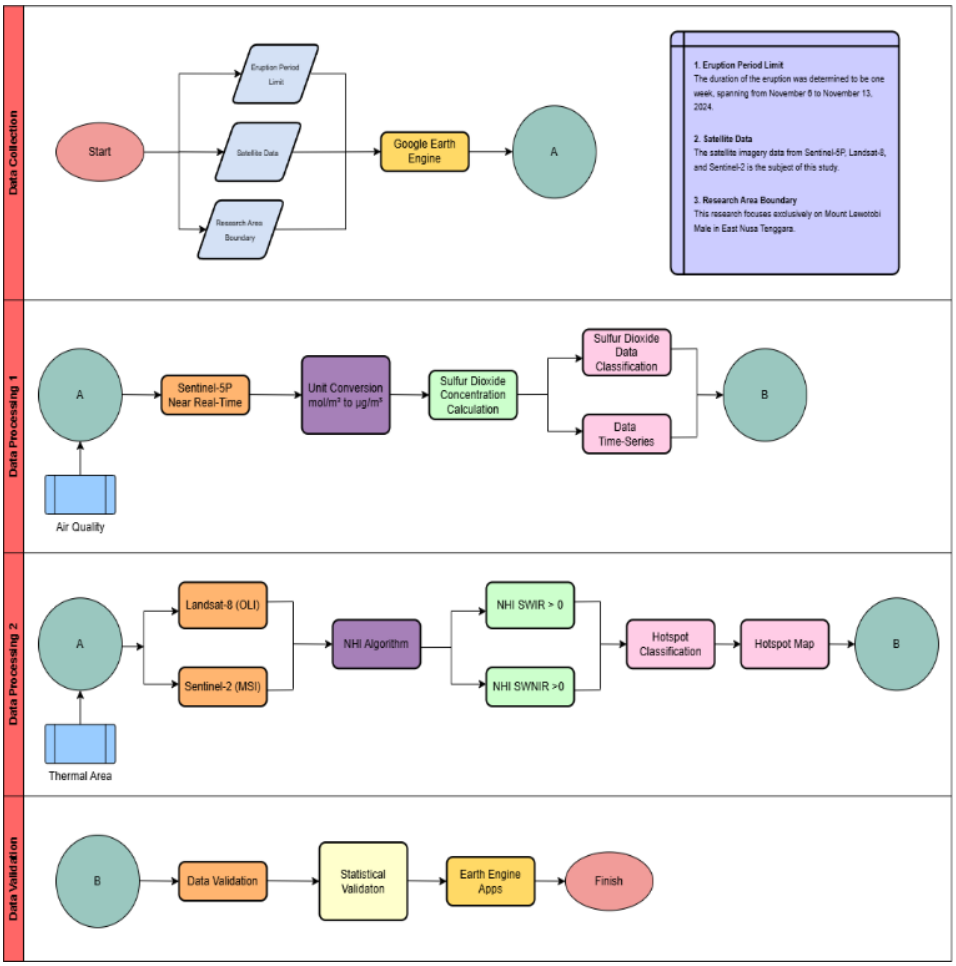


Figure 2. Research flow chart

$$NHI_{SWIR} = \frac{L_{SWIR2} - L_{SWIR1}}{L_{SWIR2} + L_{SWIR1}} \quad (1)$$

$$NHI_{SWNIR} = \frac{L_{SWIR1} - L_{NIR}}{L_{SWIR1} + L_{NIR}} \quad (2)$$

High NHI values indicate an increase in thermal energy emissions, which can be used to spatially identify volcanic hotspot. This method was adapted from a previous study by [7] and has been proven effective in detecting thermal changes on the ground surface due to volcanic activity. To ensure the accuracy of $SO_2$ detection and mapping results as well as thermal anomalies, this study uses two external validation datasets. MIROVA (Middle InfraRed Observation of Volcanic Activity) serves as an independent data validation source in this study by providing daily, satellite-derived thermal anomaly information using data from MODIS and VIIRS sensors. MIROVA is a globally recognized monitoring system, employs continuous monitoring and quantification of volcanic thermal activity based on middle infrared emissions, providing consistent, standardized, and widely recognized datasets [12]. Integration of MIROVA data as a validation step facilitates a comparison between the thermal anomalies identified through the Normalized Hotspot Indices (NHI) algorithm processed from Sentinel-2 and Landsat-8 imagery within Google Earth Engine (GEE) and the anomalies detected by MIROVA. This cross-comparison enhances the reliability and credibility of the NHI-based hotspot detection results by ensuring that the identified hotspots correspond to independently observed volcanic thermal signals. The second dataset is $SO_2$ monitoring data from NASA, which is used to verify the results of $SO_2$ column extraction from Sentinel-5P images. This data is highly useful in monitoring trends and the spatial extent of gas plume distribution during the eruption period of Mount Lewotobi Laki-Laki, thereby enhancing the reliability of spatial-temporal analysis results of volcanic gas emissions in this study. This integrated approach offers advantages in

producing more accurate spatial mapping of the environmental impacts of the Mount Lewotobi Laki-Laki eruption.

## III. RESULT AND DISCUSSION

### *3.1 Levels of Sulfur Dioxide Content Due to Eruptions*

Image processing obtained from Sentinel-5P was carried out using a cloud-based platform, namely GEE. The type of band used to determine sulfur dioxide content is "SO2_column_number_density," which allows for analysis of the horizontal and vertical distribution of this gas. The analyzed area is limited to a radius of 50 km from Mount Lewotobi Laki-Laki at a tropospheric height of 13 km [13]. The following are the results of the maximum daily concentration and average daily concentration at tropospheric height in Table 1.

Table 1. Data on sulfur dioxide levels in the air during the eruption period

| No | Date | Maximum Daily Value (µg/m³) | Average Daily Value (µg/m³) |
|---|---|---|---|
| 1 | 06/11/2024 | 16.183 | 2.618 |
| 2 | 07/11/2024 | 241.635 | 37.292 |
| 3 | 08/11/2024 | 39.72 | 16.621 |
| 4 | 09/11/2024 | 300.831 | 71.928 |
| 5 | 10/11/2024 | 170.675 | 22.254 |
| 6 | 11/11/2024 | 133.722 | 18.959 |
| 7 | 12/11/2024 | 29.262 | 2.439 |

Based on Table 1, image processing results show that the maximum concentration of sulfur dioxide was recorded on November 9, 2024, with a value of 300.831 µg/m³. Meanwhile, the highest daily average value for $SO_2$ during that period was 71.928 µg/m³. Conversely, the lowest daily concentration was recorded on November 6, 2024, at 16.183 µg/m³, and the lowest daily average was recorded at 2.483 µg/m³. Based on the analysis of the graph in Figure 3, there was a significant increase in $SO_2$ concentration from November 6 to November 9, 2024. This increase indicates that the eruption of Mount Lewotobi Laki-Laki occurred repeatedly, with the peak eruption recorded on November 9, 2024. Subsequently, there was a significant decrease in $SO_2$ concentration recorded during the period from November 10 to 12, 2024. This decrease indicates a reduction in volcanic activity intensity following the eruption peak. Figure 4 below shows the distribution of sulfur dioxide from Mount Lewotobi.

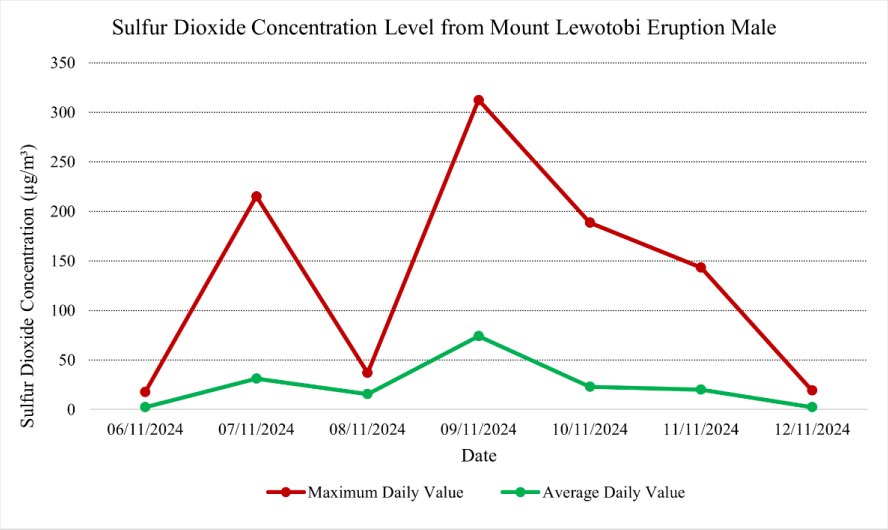


Figure 3. Graph showing the measurement of sulfur dioxide content during the eruption period

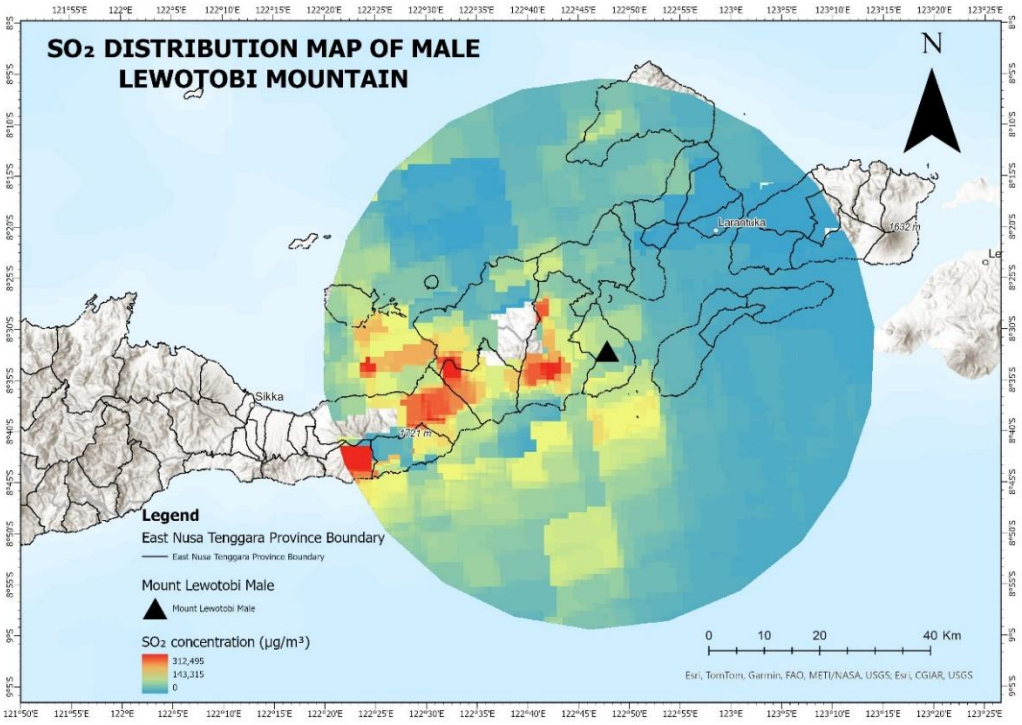


Figure 4. Map of sulfur dioxide distribution obtained during the eruption period

### *3.2 Analysis of Hotspot Distribution in Lava Eruptions*

The distribution of hot pixels generated by the eruption of Mount Lewotobi Laki-Laki was analyzed using Landsat-8 (OLI) and Sentinel-2 (MSI) satellite imagery. Hotspot detection was performed using the Normalized Hotspot Indices (NHI) algorithm, which utilizes a combination of SWIR (Shortwave Infrared) and NIR (Near Infrared) to distinguish hot pixels from surrounding areas, thereby mapping regions with significant thermal activity resulting from the eruption. NHI measurements were conducted in the area surrounding the eruption of Mount Lewotobi Laki-Laki, with the highest hotspot recorded on November 13, 2024. The following is a graph showing the number of hot pixels measured by Landsat-8 and Sentinel-2.

The graph shown in Figure 5 shows the total number of hot pixels measured from Landsat-8 imagery, with a result of 51 hotspots detected. Meanwhile, measurements taken using Sentinel-2 (Figure 6) on the same date showed 265 hotspots. The area affected by the lava eruption was calculated to be 106,000 m² based on the number of hot spots generated. This difference in the number of hot pixels is due to the difference in spatial resolution between the two satellites, where Sentinel-2 has a resolution of 20 meters, while Landsat-8 has a resolution of 30 meters, as well as the difference in wavelength used for data processing.

The comparison of wavelengths used to measure the intensity of hot pixels is also shown in Figures 7 and 8. Measurements using SWIR on Landsat-8 (Figure 7) show significant radiation at wavelengths of 1600 nm (SWIR 1) and 2200 nm (SWIR 2), with total radiance values of $519.793\ W \cdot m^{-2} \cdot sr^{-1} \cdot \mu m^{-1}$ and $686.25\ W \cdot m^{-2} \cdot sr^{-1} \cdot \mu m^{-1}$. Meanwhile, measurements with Sentinel-2 (Figure 8) show higher radiance values, with total radiance at wavelengths of 1600 nm and 2200 nm of $3569.715\ W \cdot m^{-2} \cdot sr^{-1} \cdot \mu m^{-1}$ and $4550.083\ W \cdot m^{-2} \cdot sr^{-1} \cdot \mu m^{-1}$, indicating greater sensitivity to hot pixels.

Hotspot measurement data obtained from Landsat-8 and Sentinel-2 were then validated with data obtained from MIROVA, which can be accessed through the MIROVA Web site. For example, on November 13, 2024, measurements using GEE on Landsat-8 imagery resulted in 51 hotspots, while MIROVA recorded 227 hotspots. Similarly, Sentinel-2 measurements using GEE resulted in 265 hotspots, while MIROVA recorded 444 hotspots on the same date. The difference between these measurements is related to the differences in data acquisition characteristics between the two platforms

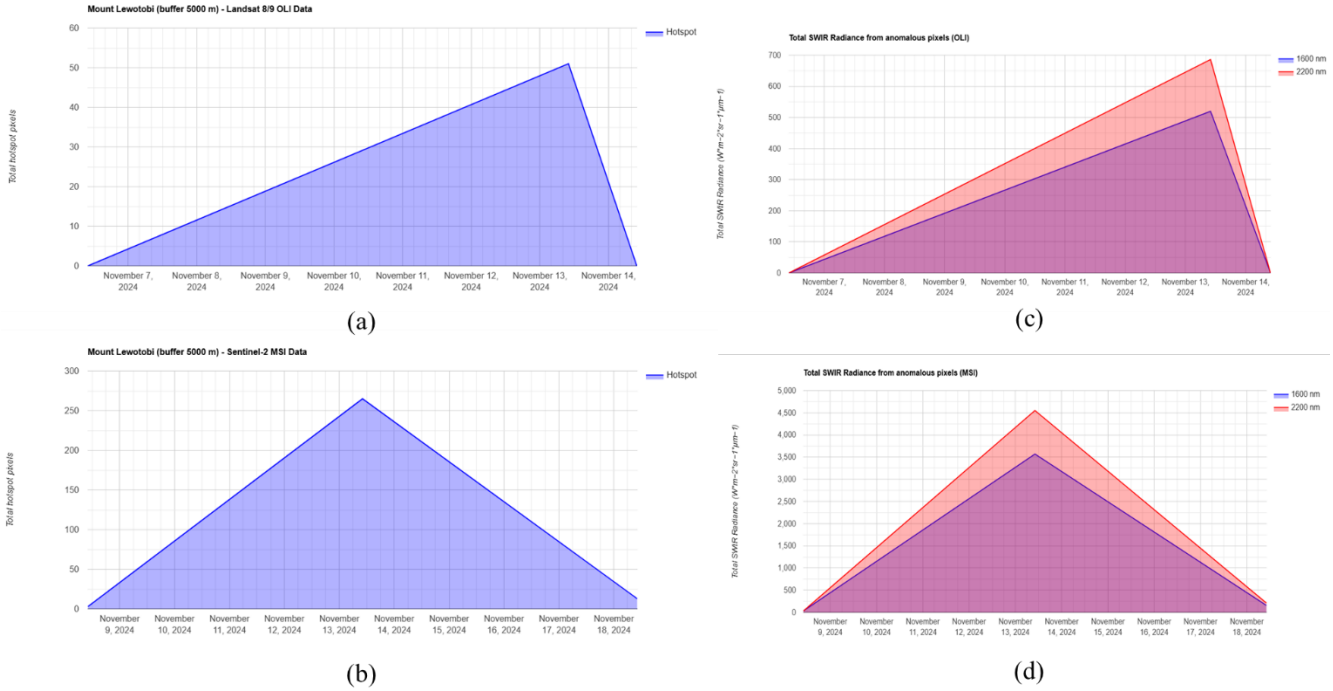


Figure 5. (a) Hotspots number based on Landsat -8 data , (b) Hotspots number based on Landsat -8 data, (c) Total SWIR radiance based on OLI pixel and (d) Total SWIR radiance based on MSI pixel

Furthermore, statistical calculations were performed using Welch's t-statistic equation to test for significant differences between measurements obtained from GEE and MIROVA. The results of the calculations can be seen in the table below, which shows that the p-value for both Landsat-8 and Sentinel-2 data is greater than α (0.05). For Landsat-8 data, the p-value was 0.409, while for Sentinel-2, the p-value was 0.456. Based on the two-tailed test, the null hypothesis $H_0$, which states that there is no significant difference between the measurements produced by GEE and MIROVA, can be accepted. The test results are shown in the table below.

Table 2. Validation of hotspot comparison measurements between Sentinel-2 and MIROVA

| Parameter | Sentinel-2 (GEE) | Sentinel-2 (MIROVA) |
|---|---|---|
| Mean | 9.266666667 | 22.6 |
| Variance | 2338.547126 | 7107.627586 |
| Observations | 30 | 30 |
| Hypothesized Mean Difference | 0 | |
| df | 46 | |
| t Stat | -0.751400322 | |
| P(T<=t) two-tail | 0.456238995 | |
| t Critical two-tail | 2.012895599 | |

Table 3. Validation of hot pixel comparison measurements between Landsat-8 and MIROVA

| Parameter | Landsat-8 (GEE) | Landsat-8 (MIROVA) |
|---|---|---|
| Mean | 1.7 | 8.166666667 |
| Variance | 86.7 | 1713.316092 |
| Observations | 30 | 30 |
| Hypothesized Mean Difference | 0 | |
| df | 32 | |
| t Stat | -0.834839345 | |
| P(T<=t) two-tail | 0.409997806 | |
| t Critical two-tail | 2.036933343 | |

The table above shows that there are no significant differences in the hotspot measurements obtained from both Landsat-8 and Sentinel-2 data compared to MIROVA validation data. These results demonstrate the consistency of measurements between the two platforms, both in terms

of spatial resolution and the data processing methods used. On the other hand, continuing the analysis of validated hotspot measurements, the visualization of measured hotspot areas using Landsat-8 and Sentinel-2 imagery shows variations in recorded intensity. Based on the data acquisition results from both satellite images, there are differences in the distribution of heat intensity, ranging from high to moderate to low.

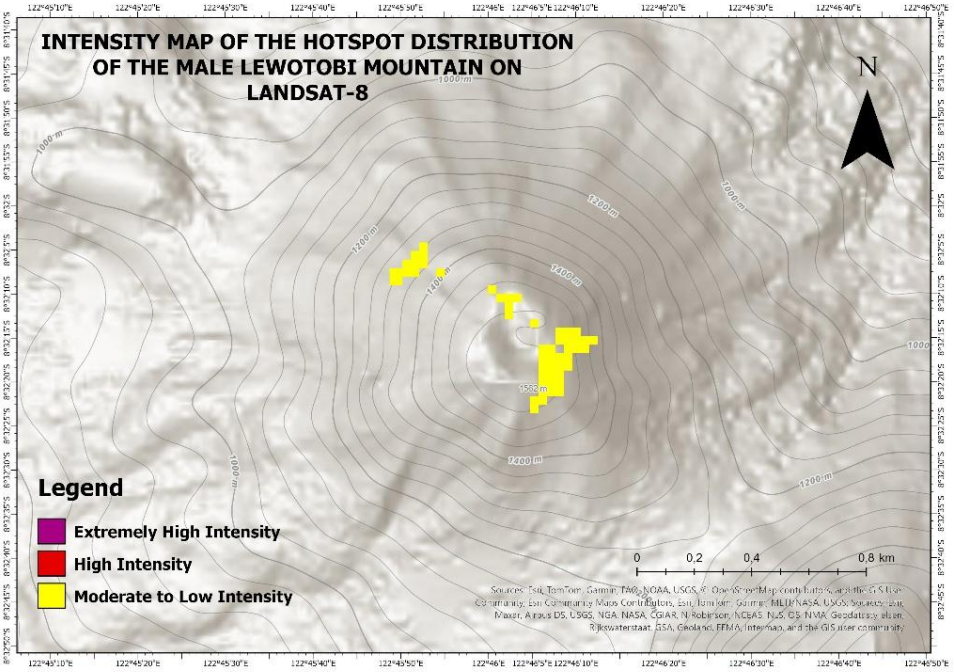


(a)

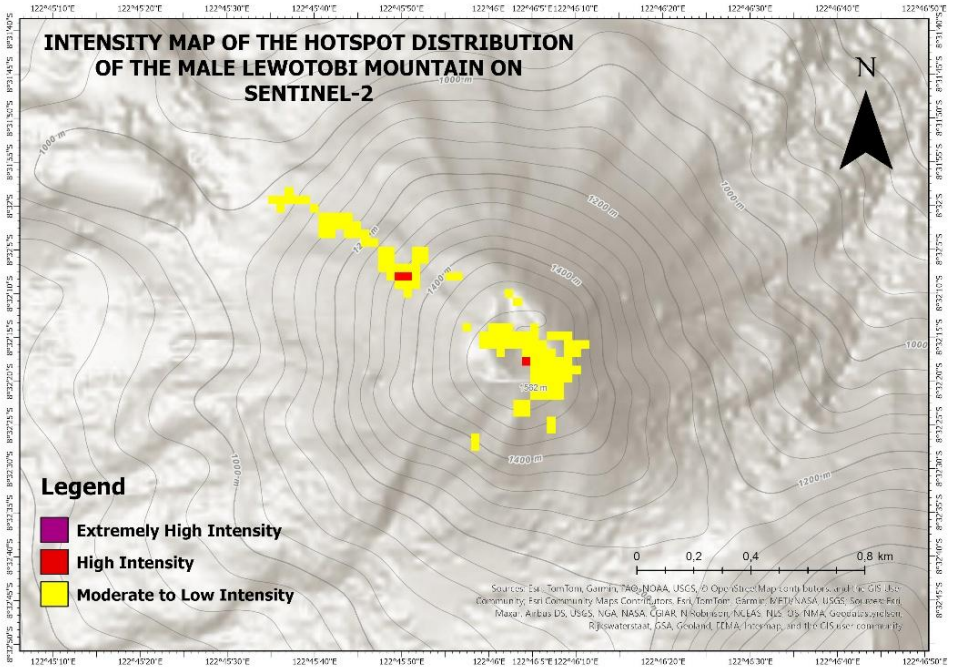


(b)

Figure 6. Hotspots intensity map from (a) Landsat-8 data and (b) Sentinel-2 data

### *3.3 Analysis of the Increase in Sulfur Dioxide Content on the Number of Hot Pixels Due to Lava Eruption*

Sulfur dioxide ($SO_2$) is a volcanic gas released during volcanic activity, and an increase in the concentration of this gas is an indicator of significant volcanic activity [14]. Hot pixels detected in the eruption area are directly related to the lava flow produced by the eruption process [9]. The interaction of lava with the surrounding environment can affect the number of hotspot detected by satellite imagery. In analyzing the effect of increased sulfur dioxide content on the number of hot pixels, data from Sentinel-5P, Sentinel-2, and Landsat-8 were combined to produce a more comprehensive picture.

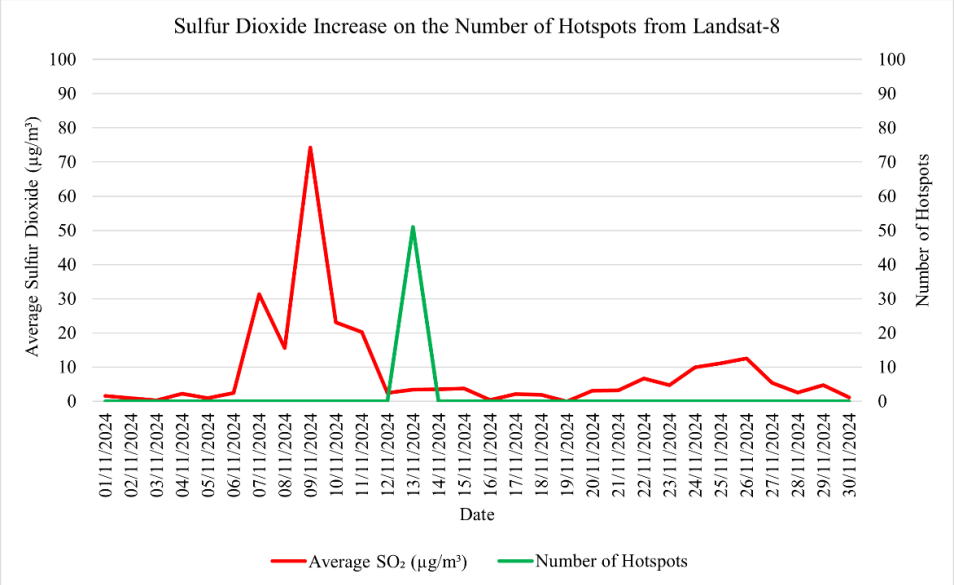


(a)

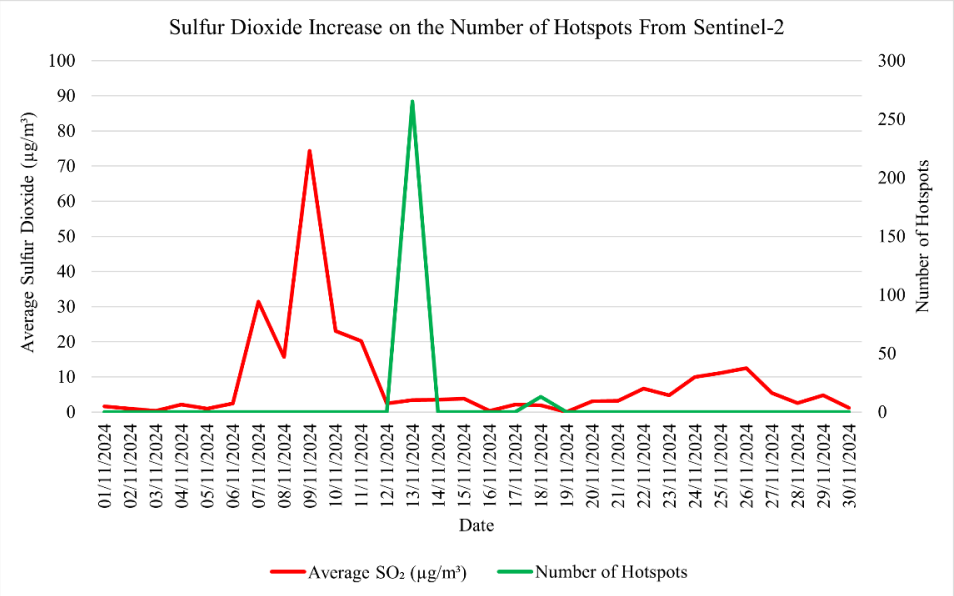


(b)

Figure 7. Comparison of the number of hot pixels to the increase in sulfur dioxide content from Sentinel-2 data

Figures 7 show the effect of increased sulfur dioxide on the number of hotspots detected from Sentinel-5P, Sentinel-2, and Landsat-8 data. Figure 9 highlights the difference between Sentinel-5P and Landsat-8 data, where Sentinel-5P has a faster acquisition frequency (2 days) compared to Landsat-8, which only acquires data every 16 days, resulting in data with higher variability. Meanwhile, Figure 12 shows that on November 9, 2024, sulfur dioxide levels peaked at over 71.928 µg/m³, while Sentinel-2 data on November 13, 2024, recorded around 265 hot pixels. An increase in hot pixels was also observed on November 17–18, 2024, albeit with lower intensity, indicating a relationship between the increase in sulfur dioxide and the eruptive activity of Mount Lewotobi Laki-Laki.

To validate the increase in sulfur dioxide against the number of hot pixels, a statistical test was conducted using Pearson's correlation test. This test aims to measure the linear relationship between two quantitative variables, namely the sulfur dioxide content in the air and the number of hot pixels detected due to the eruption of Mount Lewotobi Laki-Laki. This is evidenced by figure below.

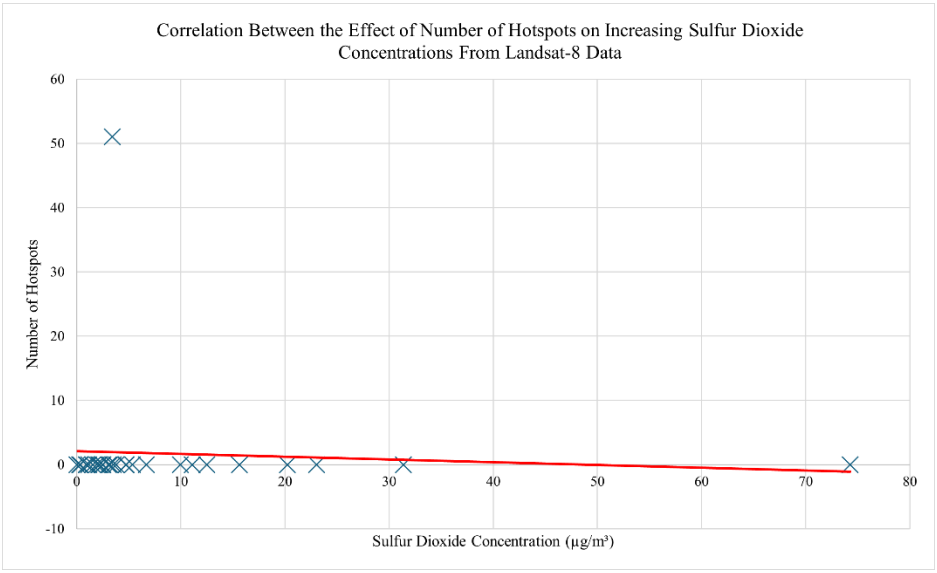


(a)

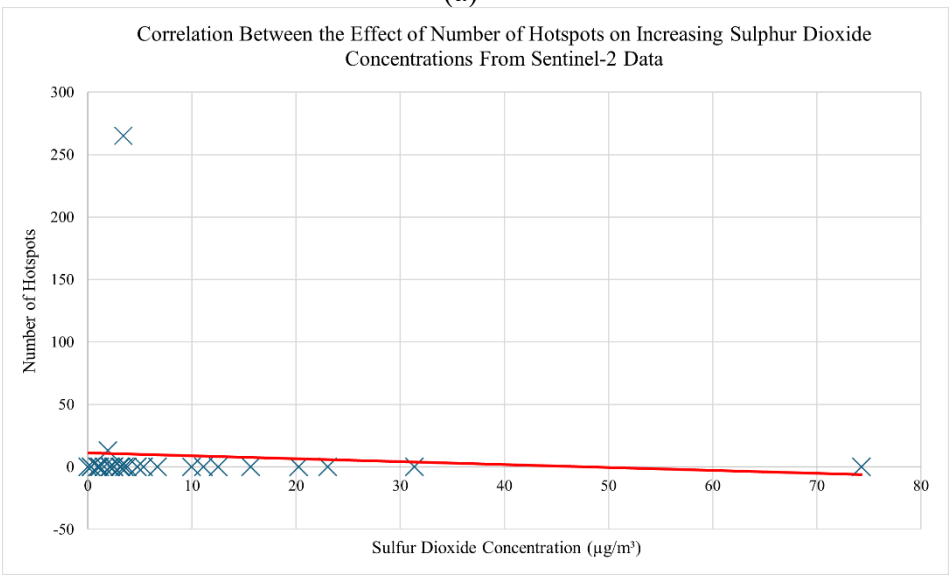


(b)

Figure 8. Correlation between the number of hotspot and the increase in sulfur dioxide levels from Sentinel-2 data

Figure 8 shows that the Pearson correlation results indicate a weak negative relationship between the two variables, with values of -0.0764 for Landsat-8 and -0.0832 for Sentinel-2, indicating that the increase in sulfur dioxide is not significantly related to the number of hotspots detected. $SO_2$ emissions are determined by volcanic degassing, which can occur independently of surface thermal manifestations, such as fresh lava flows or high-temperature vents detected as hotspots. Temporal mismatches between peak degassing events and peak thermal activity, as well as differences in spatial scale where Sentinel-5P records atmospheric gas concentrations over broader areas, while Landsat-8 and Sentinel-2 detect localized surface heat further contribute to the weak statistical relationship. Furthermore, atmospheric conditions, including wind dispersion and cloud cover, have the potential to obscure or redistribute gas plumes, potentially reducing the apparent correlation with surface thermal signatures. To further confirm these results, a t-statistic test was also conducted using the $H_0$ and $H_1$ hypotheses. The absolute t-test results from the Landsat-8 data were 0.4057 and 2.3380 for the Sentinel-2 data measurements. Based on the measurements obtained, when compared with the t-table value with a degrees of freedom of 95%, the t-table value obtained was 2.048. The results obtained show that both data values are smaller than the t-table data used for testing, leading to the conclusion that there is no significant relationship between sulfur dioxide concentrations and the number of hotspots from the lava eruption of Mount Lewotobi Laki-Laki.

This study focuses on monitoring sulfur dioxide ($SO_2$) emissions and thermal anomalies caused by eruptions using data from Sentinel-5P, Sentinel-2, and Landsat-8, processed through Google Earth Engine. For comparison, the study by [15] , related to the eruption of Mount Mauna Loa in Hawaii, which occurred in November-December 2022, used GOES-R ABI, Sentinel-2, and Landsat 8/9 to monitor thermal anomalies and lava flows, as well as volcanic gas emissions. GOES-R ABI provides very high temporal resolution and enables real-time monitoring of volcanic activity, with a focus on lava flows and volcanic radiative power (VRP) [16].

In this regard, although both studies focused on monitoring volcanic activity, there were significant differences in the methods and platforms used. In this study, Sentinel-5P data was used to detect $SO_2$ emissions with lower spatial resolution (~7×3.5 km), while GOES-R was used in the Mauna Loa study for thermal and gas monitoring with very high data acquisition frequencies. Although both studies use Normalized Hotspot Indices (NHI) to monitor thermal anomalies, the study on Mount Lewotobi utilizes Sentinel-2 (20 m) and Landsat-8 (30 m), providing higher spatial resolution compared to the Mauna Loa study, which uses the lower resolution of GOES-R ABI. This highlights a significant difference in spatial resolution quality, contributing new insights into thermal monitoring with improved spatial resolution and more detailed hotspot mapping.

In addition, the use of GEE in this study provides an integrated platform for efficient and large-scale spatial data processing, enabling long-term $SO_2$ analysis with more detailed spatial resolution. Therefore, differences in the selection of platforms and analysis techniques provide new depth in monitoring volcanic activity in tropical regions, which has not been widely explored before.

## IV. CONCLUSION

Based on the results of the research and data processing that has been carried out, it can be concluded that air quality affected by sulfur dioxide concentrations can be analyzed using the Google Earth Engine application. Computational results indicate that the maximum sulfur dioxide concentration recorded was 300.831 µg/m³ on November 9, 2024, with an average daily concentration of 71.928 µg/m³. The lowest concentration was recorded on November 6, 2024, at 16.183 µg/m³ and a daily average of 2.439 µg/m³, with the detected spread of sulfur dioxide extending from east to west across the Nusa Tenggara Timur region. In addition, hotspot measurements from the eruption of Mount Lewotobi Laki-Laki were conducted using Sentinel-2 and Landsat-8 satellite imagery. Sentinel-2 data recorded a maximum of 265 hotspots, while Landsat-8 recorded 51 hotspots. The detected hot area was estimated to be around 106,000 m², with the difference in the number of detected hotspots due to the difference in spatial resolution between the two satellites.

Validation and correlation tests were performed on the hotspot measurement data from Sentinel-2 and Landsat-8 images using the Google Earth Engine computational method, with measurement data from MIROVA as a comparison. The t-statistic test results showed that the p-value for Landsat-8 was 0.409, while for Sentinel-2 it was 0.456. By comparing these values to the significance level ($\alpha = 0.05$), it can be concluded that there is no significant difference between the two image datasets in determining the number of hotspots compared to MIROVA. Furthermore, the results of the Pearson correlation test show a negative relationship between sulfur dioxide ($SO_2$) concentration and the number of hotspots, with a correlation value of -0.0764 for Landsat-8 and -0.0832 for Sentinel-2. This indicates that an increase in $SO_2$

concentration tends to be followed by a decrease in the number of hotspots, although the correlation is weak.

Testing using t-statistics on the relationship between $SO_2$ and the number of hotspots yielded an absolute t-value of 0.4057 for Landsat-8 and 2.3380 for Sentinel-2. With a t-table value of 2.048 (at a significance level of 95%), it can be concluded that there is no significant relationship in the Landsat-8 measurements. However, this is not the case with Sentinel-2, where the t-value exceeding the t-table indicates a significant relationship between sulfur dioxide concentrations in the air and the number of hotspots caused by the lava eruption of Mount Lewotobi Laki-Laki. The present study proposes a methodology for the practical monitoring of volcanic activity across large spatial and temporal scales. This methodology combines the Normalized Hotspot Indices (NHI) algorithm with $SO_2$ concentration analysis, thereby overcoming many traditional limitations associated with ground-based observation networks. On a global scale, this methodology can support the development of early warning systems and risk assessments by providing near-real-time insights into volcanic thermal activity and gas emissions. These insights are critical for disaster preparedness, aviation safety, and public health protection.

Further research development should focus on enhancing the accuracy and applicability of volcanic monitoring by integrating additional satellite sensors with higher spatial, temporal, and spectral resolution to complement existing analyses from Landsat-8, Sentinel-2, and Sentinel-5P. The incorporation of ground-based observations would facilitate more robust validation of satellite-derived hotspot and SO2 detection, thereby enhancing the reliability of interpretation. Consequently, the development of near-real-time dashboards or alert systems based on this integrated approach would considerably enhance its operational value for disaster risk reduction, aviation safety, and public communication at both local and global scales.

## ACKNOWLEDGEMENT

This research utilizes data from the Sentinel-5P satellite mission, provided by the European Space Agency (ESA) and accessed through the Google Earth Engine (GEE) platform. We gratefully acknowledge the Copernicus Programme for providing free and open access to satellite data, and the Google Earth Engine team for enabling large-scale geospatial data analysis.

## REFERENCES

[1] E. Hariyono and L. S, "The Characteristics of Volcanic Eruption in Indonesia," in *Volcanoes - Geological and Geophysical Setting, Theoretical Aspects and Numerical Modeling, Applications to Industry and Their Impact on the Human Health*, InTech, 2018. doi: 10.5772/intechopen.71449.

[2] P. C. Pandey, "Highlighting the role of earth observation Sentinel5P TROPOMI in monitoring volcanic eruptions: a report on Hunga Tonga, a Submarine Volcano," *Remote Sensing Letters*, vol. 13, no. 9, pp. 912–923, 2022, doi: 10.1080/2150704X.2022.2106799.

[3] F. Marchese and N. Genzano, "Global volcano monitoring through the Normalized Hotspot Indices (NHI) system," *J Geol Soc London*, vol. 180, no. 1, Jan. 2023, doi: 10.1144/jgs2022-014.

[4] C. Corradino, P. Jouve, A. La Spina, and C. Del Negro, "Monitoring Earth's atmosphere with Sentinel-5 TROPOMI and Artificial Intelligence: Quantifying volcanic SO2 emissions," *Remote Sens Environ*, vol. 315, Dec. 2024, doi: 10.1016/j.rse.2024.114463.

[5] H. Eskes *et al.*, "Sentinel-5 precursor/TROPOMI Level 2 Product User Manual Nitrogendioxide document number : S5P-KNMI-L2-0021-MA," 2022.

[6] A. Inness *et al.*, "Evaluating the assimilation of S5P/TROPOMI near real-time SO2columns and layer height data into the CAMS integrated forecasting system (CY47R1), based on a case study of the 2019 Raikoke eruption," *Geosci Model Dev*, vol. 15, no. 3, pp. 971–994, Feb. 2022, doi: 10.5194/gmd-15-971-2022.

[7] G. Mazzeo, M. S. Ramsey, F. Marchese, N. Genzano, and N. Pergola, "Implementation of the NHI (Normalized hot spot indices) algorithm on infrared aster data: Results and future perspectives," *Sensors*, vol. 21, no. 4, pp. 1–16, Feb. 2021, doi: 10.3390/s21041538.

[8] M. Drusch *et al.*, "Sentinel-2: ESA's Optical High-Resolution Mission for GMES Operational Services," *Remote Sens Environ*, vol. 120, pp. 25–36, May 2012, doi: 10.1016/j.rse.2011.11.026.

[9] S. Valade *et al.*, "Towards global volcano monitoring using multisensor sentinel missions and artificial intelligence: The MOUNTS monitoring system," *Remote Sens (Basel)*, vol. 11, no. 13, Jul. 2019, doi: 10.3390/rs11131528.

[10] V. Ihlen, "Landsat 8 (L8) Data Users Handbook," 2019.

[11] J. Wei *et al.*, "Global aerosol retrieval over land from Landsat imagery integrating Transformer and Google Earth Engine," *Remote Sens Environ*, vol. 315, p. 114404, Dec. 2024, doi: 10.1016/j.rse.2024.114404.

[12] D. Coppola *et al.*, "Thermal Remote Sensing for Global Volcano Monitoring: Experiences From the MIROVA System," *Front Earth Sci (Lausanne)*, vol. 7, Jan. 2020, doi: 10.3389/feart.2019.00362.

[13] N. Theys *et al.*, "A sulfur dioxide Covariance-Based Retrieval Algorithm (COBRA): application to TROPOMI reveals new emission sources," *Atmos Chem Phys*, vol. 21, no. 22, pp. 16727–16744, Nov. 2021, doi: 10.5194/acp-21-16727-2021.

[14] S. Corradini *et al.*, "Tropospheric volcanic so2 mass and flux retrievals from satellite. The etna december 2018

eruption," *Remote Sens (Basel)*, vol. 13, no. 11, Jun. 2021, doi: 10.3390/rs13112225.

[15] N. Genzano, N. Pergola, and F. Marchese, "A google earth engine tool to investigate, map and monitor volcanic thermal anomalies at global scale by means of mid-high spatial resolution satellite data," *Remote Sens (Basel)*, vol. 12, no. 19, pp. 1–22, Oct. 2020, doi: 10.3390/rs12193232.

[16] N. Genzano, F. Marchese, M. Neri, N. Pergola, and V. Tramutoli, "Implementation of robust satellite techniques for volcanoes on aster data under the google earth engine platform," *Applied Sciences (Switzerland)*, vol. 11, no. 9, May 2021, doi: 10.3390/app11094201.